ASM Handbook, Volume 15: Casting
ASM Handbook Committee, p 390-397
DOI: 10.1361/asmhba0005227

Solidification During Casting of Metal-Matrix Composites

Pradeep Rohatgi and Benjamin Schultz, University of Wisconsin—Milwaukee
Nikhil Gupta, Polytechnic Institute of New York University
Atef Daoud, Central Metallurgical Research and Development Institute

METAL-MATRIX COMPOSITES (MMCs) are engineered combinations of two or more materials in which reinforcing phases are dispersed in a metal or an alloy. Structurally, cast MMCs consist of continuous or discontinuous fibers (designated by the subscript f), whiskers (w), or particles (p) in a metal or an alloy that solidifies in the restricted spaces between the reinforcing phase (or phases) to form the bulk of the matrix. There are several cast materials, such as aluminum-silicon alloys and cast irons, that exhibit two-phase microstructure in which the volume and shape of the phases are governed by phase equilibria and that have a long history of foundry production. Modern cast MMCs differ from these traditional materials in that any selected volume, shape, and size of reinforcement can be introduced into the matrix, even beyond the permissible limits presented by the phase diagrams.

By carefully controlling the size, shape, surface properties, volume fraction, and distribution of the reinforcement and by controlling the solidification conditions, MMCs can be synthesized having a tailored set of useful engineering properties. For example, as shown in Table 1, combinations of very high specific strength and specific modulus, beyond those of conventional monolithic alloys, are achievable. Table 2 summarizes the applications of several commonly used MMCs and the properties that make them suitable for their applications. Microstructural design and synthesis procedures have been developed to achieve unique combinations of properties, including improved elevated-temperature and fatigue strengths, increased damping ability, tailored electrical and thermal conductivities, reduced wear rates, and targeted coefficients of thermal expansion. These tailored properties provide opportunities for a variety of new applications for MMCs that were not possible using conventional materials. For more information about MMC types and their applications, see the

Table 1 Specific strength and specific modulus of some metal matrices, reinforcements, and metal-matrix composites

Material	Amount of fiber reinforcement, vol%	Specific strength, N · m/kg	Specific modulus, N · m/kg
Al-Li/Al_2O_3			
0°	60	20,000	7.59×10^7
90°	60	4,986–6,000	4.406×10^7
Ti-6Al-4V/SiC			
0°	35	45,337	7.77×10^7
90°	35	10,622	...
Mg/carbon (Thornel)	38	28,333	...
Al/carbon	30	28,163	6.53×10^7
6061 Al	...	11,481	2.53×10^7
2014 Al	...	17,143	2.59×10^7
$SiC_{(f)}$	100	78,431	1.567×10^8
$SiC_{(w)}$	100	6.67×10^5	2.19 to 3.29×10^8
$Al_2O_{3(f)}$	100	50,000	1.175×10^8
$B_{(f)}$	100	1.538×10^5	1.62×10^8
$C_{(f)}$	100	1.618×10^5	1.35×10^8
$Be_{(f)}$	100	59,459	1.68×10^8
$W_{(f)}$	100	14,974	1.79×10^7
Al/boron			
0°	50	56,604	7.92×10^7
90°	50	5,283	5.66×10^7
Al/SiC			
0°	50	8,803	1.092×10^8
90°	50	3,697	...

Table 2 Selected potential applications of cast metal-matrix composites

Composite	Applications	Special features
Aluminum/graphite	Bearings	Cheaper, lighter, self-lubricating, conserve Cu, Pb, Sn, Zn, etc.
Aluminum/graphite, aluminum/α-Al_2O_3, aluminum/SiC-Al_2O_3	Automobile pistons, cylinder liners, piston rings, connecting rods	Reduced wear, antiseizing, cold start, lighter, conserves fuel, i mproved efficiency
Copper/graphite	Sliding electrical contacts	Excellent conductivity and antiseizing properties
Aluminum/SiC	Turbocharger impellers	High-temperature use
Aluminum/glass or carbon microballoons	...	Ultralight materials
Magnesium/carbon fiber	Tubular composites for space structures	Zero thermal expansion, high-temperature strength, good specific strength and specific stiffness
Aluminum/zircon, aluminum/SiC, aluminum/silica	Cutting tools, machine shrouds, impellers	Hard, abrasion-resistant materials
Aluminum/char, aluminum/clay	Low-cost, low-energy materials	...

article "Synthesis and Processing of Cast Metal-Matrix Composites and Their Applications" in this Volume.

The matrix alloy in cast MMCs solidifies in the restricted space between the reinforcing phase to form the bulk of the matrix. The solidification microstructure of the matrix is refined and modified due to the presence of fibers and/or particles, providing a possible means of controlling solute microsegregation within the microstructure, macrosegregation of reinforcements in the casting, and the grain size in the matrix. The microstructure of the matrix surrounding the reinforcements and the nature of the interface between reinforcements and the matrix are important contributors to the overall MMC properties. The reactions at the solid-liquid interface and the nucleation and growth of primary and secondary phases around reinforcements influence the microsegregation and nanosegregation of reinforcements within the matrix microstructure.

Incorporation of Reinforcements

Most ceramics are not wetted or are poorly wetted by molten metals, so the intimate contact between reinforcement and alloy can only be promoted by artificially inducing wettability or by using external forces to overcome the thermodynamic surface energy barrier and viscous drag effects. Mixing techniques generally used for introducing and homogeneously dispersing a discontinuous phase in a melt are:

- Addition of particles to a vigorously agitated, fully or partially molten melt (Ref 1–4)
- Injection of discontinuous phase into the melt with an injection gun (Ref 5)
- Dispersion of pellets or briquettes into a mildly agitated melt (Ref 6)
- Addition of powders to an ultrasonically agitated melt
- Addition of powders to an electromagnetically stirred melt
- Centrifugal dispersion of particles in a melt
- Infiltration of loose or packed beds/preforms of reinforcements by molten alloys

Reinforcement-Metal Wettability

Wetting between molten alloys and dispersoids is desirable from the standpoint of ease of fabrication, dispersion of particles, and property-performance relationships (Ref 7, 8). Improvement in wetting between the matrix and the reinforcing phase is also important to minimize or eliminate porosity and to help the reinforcement function as a nucleation catalyst for the matrix microstructure.

The wetting properties of ceramics by liquid metals are governed by a number of variables, including heat of formation, stoichiometry, and valence electron concentration. High temperature and long contact times promote wettability due to interfacial reactions, resulting in reduced contact angle between the ceramic phase and the melt. The work of adhesion between a ceramic and a melt decreases with increasing heat of formation of carbides. A high energy of formation for a stable carbide implies strong interatomic bonds and correspondingly weak interaction with melts. This leads to a high interfacial energy and a small work of immersion, resulting in poor wetting. High valence electron concentration generally implies lower stability of carbides and improved wettability of ceramics by metals. Hence, optimization of processing parameters based on thermodynamics and kinetics can result in higher-quality MMCs.

Magnesium/graphite, aluminum/graphite, and several other fiber-reinforced composites are valuable structural materials because they combine high specific strength and stiffness with a near-zero coefficient of thermal expansion and high electrical and thermal conductivities. Wetting and bonding between the fiber and the metal in these systems is induced by the deposition of a thin layer of titanium and boron or SiO_2 onto the fibers (Ref 9).

Solidification Processing of MMC

In solidification processing of composites, liquid metal is combined with the reinforcement phase and solidified in a mold. The solidification processes of composite synthesis can be divided into two main classes: stir mixing and melt infiltration. (For more information, see *Composites,* Volume 21, *ASM Handbook*.)

Stir Mixing. In stir mixing, the reinforcement phase is added to the melt, and the mixture is stirred with the help of either a mechanical stirrer (Ref 10) or a high-intensity ultrasonic device (Ref 11, 12). This action disperses the reinforcing phase throughout the melt. The melt-particle slurry can be cast either by conventional foundry techniques, such as gravity, pressure die, or centrifugal casting, or by novel techniques such as squeeze casting (liquid forging), spray codeposition, melt spinning, or laser-engineered net shaping processing. Many of these casting techniques are covered in detail in other articles in this volume some typical squeeze casting parameters are shown in Table 3. Rohatgi et al. (Ref 7) have studied the thermodynamics and kinetics of transfer of particulate and fibrous reinforcements into the melt and the solidification of melt into a composite solid phase. This information has been used to design processes that are used to make different cast MMCs. Figure 1 shows typical microstructures of particle-dispersed composites produced by the stir-casting method (Ref 8).

Stir mixing and casting is now used for large-scale production of particle-reinforced MMCs (Ref 14, 15). Various metals, such as aluminum, magnesium, nickel, and copper, have been employed as the matrix, and a wide variety of reinforcements, such as SiC, graphite, SiO_2, Al_2O_3, Si_3N_4, and $ZrSiO_4$, have been added as reinforcements. The study of cast composites has added considerable understanding to the solidification of conventional monolithic castings, especially issues related to the effects of inclusions on the fluidity, viscosity, nucleation, growth, particle settling, and particle pushing.

Table 3 Typical casting conditions for SiC fiber-reinforced aluminum and aluminum alloy (Al-4.5Cu, Al-11.8Si, and Al-4.8Mg) composites

Type of composite	Metal mold temperature, K	Time between pouring and pressurizing, s	Applied pressure		Pressure time, s	Casting temperature, K
			MPa	ksi		
Plate type	573	10	49	7.1	90	1073
Tubular type	573	13	40	5.8	90	1073

Source: Ref 13

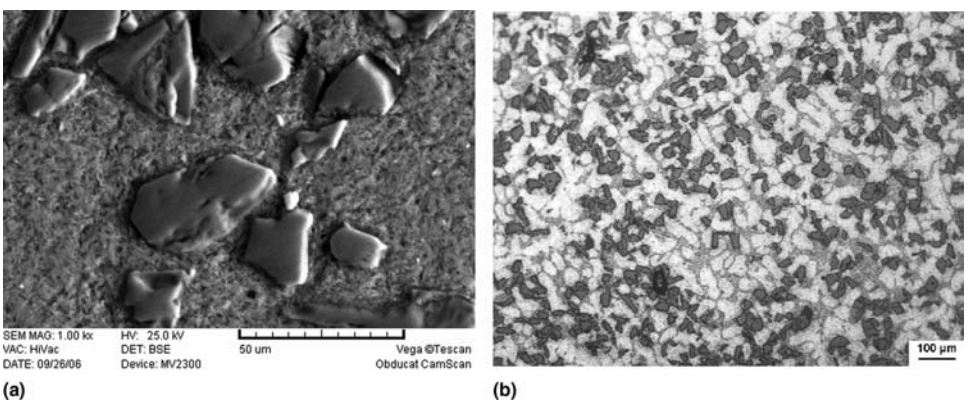

Fig. 1 Microstructures of typical cast metal-matrix composites made by stir casting. (a) A356/20wt%Al_2O_3. (b) A356/15wt%SiC_p

In stir-mixed slurries of melts and reinforcements, it is important to retain adequate enough fluidity in the melts to make sound castings. Generally, the fluidity of alloys decreases with increasing additions of reinforcements, and this can require changes in mold design. Reciprocal relationships between fluidity and the apparent viscosity of melt-particle suspensions have been noted in aluminum-silicon alloys, iron-carbon-sulfur alloys, and Al-4.5Cu-1.5Mg alloy/2.5 wt% flaky mica composites. The fluidity values of particle-filled composite melts are generally adequate for making gravity-cast composites at low volume fraction of particles, up to approximately 30 vol%. Additions of silicon carbide, alumina, graphite, mica, and other ceramic particles to aluminum alloys cause a reduction in spiral fluidity. The spiral fluidity of these alloys decreases linearly with increasing particle surface area per unit weight. The fluidity of composite slurries decreases with decreases in the temperature. The fluidity of composite melts also depends on the shape, size, flocculation, and segregation of particles in the melt.

Infiltration Process. In this process, liquid metal is infiltrated through the narrow crevices between the fibers or particulate reinforcements, which are either in a packed bed or arranged in a preform and fixed in space (Ref 16–18). High pressure or vacuum can be used to assist the infiltration process. As the liquid metal enters between the fibers or particles during infiltration, it cools and then solidifies, producing a composite. In general, the infiltration technique is divided into three distinct operations. The first step is the preform preparation, which involves assembling the reinforcement elements together into a porous body. The second step is the infiltration process during which the liquid metal permeates the preform. The last step is the solidification of liquid metal throughout the preform. Melt infiltration can be achieved with the help of mechanical pressure (Ref 19, 20), inert gas pressure, or vacuum (Ref 21, 22). The calculations of threshold pressure needed to initiate infiltration (Young's equation) and the kinetics of infiltration (Darcy's law) are in reasonable agreement with the experiments. Table 4 lists the wetting and threshold pressures for Al/SiC and Al/B_4C composite systems. Recently, techniques of pressureless infiltration of ceramic preforms have been developed (Ref 25, 26) that allow casting of net-shaped composites.

Solidification Fundamentals

Nucleation and Growth Effects

Aluminum-silicon and aluminum-copper alloys have been extensively used as matrix materials in a wide variety of cast MMCs containing graphite and ceramic particles, carbon and glass microballoons, and discontinuous or continuous ceramic fibers (Ref 27, 28). The microstructures of these MMCs show that the primary aluminum phase tends to nucleate in the interstices between the ceramic phase, unless surface modification is carried out to promote heterogeneous nucleation on the particle or the fiber surface. The thermal conductivity and heat diffusivity of particles are generally less than those of the melt, and during the cooling process, the temperature of the particles will be higher than that of the melt. In such cases, it is difficult for the primary phase to nucleate at the particle surfaces.

Thermal analysis showed that the unreinforced alloys exhibited undercooling for primary-phase nucleation, whereas the composites generally did not show any significant undercooling. The grain size of the composites is often smaller than that of the unreinforced alloy under identical casting conditions. Solute diffusion is impeded during growth due to the barrier effects of particles. Therefore, the delayed growth from the melt gives additional time for the formation of nuclei, which can yield a refined structure. The potential of nucleation on SiC and graphite particles in aluminum-silicon alloy melts can be calculated by the chemical free energy change due to solute segregation near the particles. This finding suggests that the nucleation of primary phases on the particles is more favorable for the hypereutectic compositions than for hypoeutectic compositions. This is in agreement with the presence of primary silicon phases on the particles in hypereutectic aluminum-silicon alloy melts containing SiC or graphite particles (Fig. 2) (Ref 29) and the absence of primary α-aluminum on particles in hypoeutectic aluminum-silicon alloy melts.

Dendrite Formation and Microsegregation

The primary phase morphology and the distribution of second phases depend on the relative magnitudes of dendrite arm spacing and interfiber spacing. Figure 3(a) demonstrates the effect of fiber and platelet-type reinforcements on the solidification of aluminum-copper alloys (Ref 30). In the fiber-reinforced region, it can be seen that primary aluminum does not nucleate on the surface of fibers as expected. Primary aluminum dendrites grow outward from the region between the fibers, depositing the last freezing eutectic liquid on the fiber surfaces. A similar phenomenon occurs in SiC platelet-reinforced aluminum-copper alloys (Fig. 3b, c), where the Al-$CuAl_2$ eutectic is enriched at the SiC platelet/matrix interface, and the primary phase nucleates away from the platelets (Ref 31).

Microstructures in fiber-reinforced MMCs can be modulated in a predetermined manner by controlling interfiber spacing and cooling rate. Figure 4 (Ref 7) demonstrates microsegregation in the interfiber regions of an aluminum/carbon fiber composite, in which the carbon fibers were chilled outside of the mold. In this case, very fine-sized α-phase grains were in contact with the surfaces of graphite fibers. If the cooling rate is sufficiently high or if fiber volume fraction is sufficiently low, the matrix alloy solidifies without influence from the fibers. At sufficiently slow cooling rates, when

Table 4 Wetting characteristics and threshold infiltration pressures for aluminum/SiC and aluminum/B_4C systems

				Al/SiC			Al/B_4C		
	Temperature				Threshold infiltration pressure (P_{th})			Threshold infiltration pressure (P_{th})	
Alloy	°C	°F	Surface energy (γ), J/m^2 × 10^{-3}	Contact angle (θ), degrees	kPa	psi	Contact angle (θ), degrees	kPa	psi
Pure aluminum	700	1290	851	106.3	917	133	120.0	800	116
	800	1470	840	102.3	686.1	99.5	115.6	751.7	109
	900	1650	830	101.2	620.6	90	109.4	572.4	83
Al-2Cu	700	1290	843	106.7	934.3	135.5	116.7	786.2	114
	800	1470	832	103.7	758.5	110	114.3	710.3	103
	900	1650	822	100.2	558.5	81	110.1	586.2	85
Al-4.5Cu	800	1470	831	103.0	717.1	104	112.9	668.9	97
Al-2Mg	700	1290	767	104.6	744.7	108	115.1	675.9	98
	800	1470	757	101.2	565.4	82	98.9	241.4	35
	900	1650	747	99.3	462.0	67	95.1	137.9	20
Al-4.5Mg	800	1470	652	102.1	524.0	76	92.9	68.9	10
Al-2Si	700	1290	847	105.7	882.6	128	...	...	...
	800	1470	836	103.6	737.8	107	...	...	...
	900	1650	826	99.1	503.3	73	...	...	...
Al-4.5Si	800	1470	831	103.2	730.0	106	...	...	...

Source: Ref 23, 24

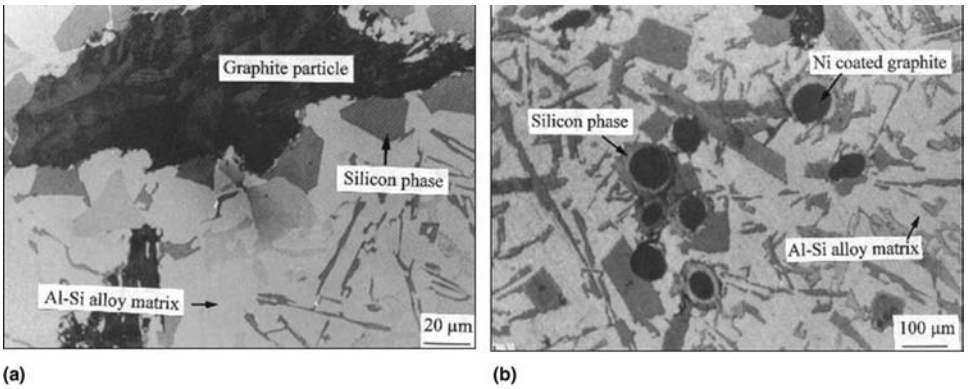

Fig. 2 Optical micrographs showing nucleation of silicon phase (a) on graphite particle and (b) on nickel-coated graphite particles in hypereutectic aluminum-silicon alloys

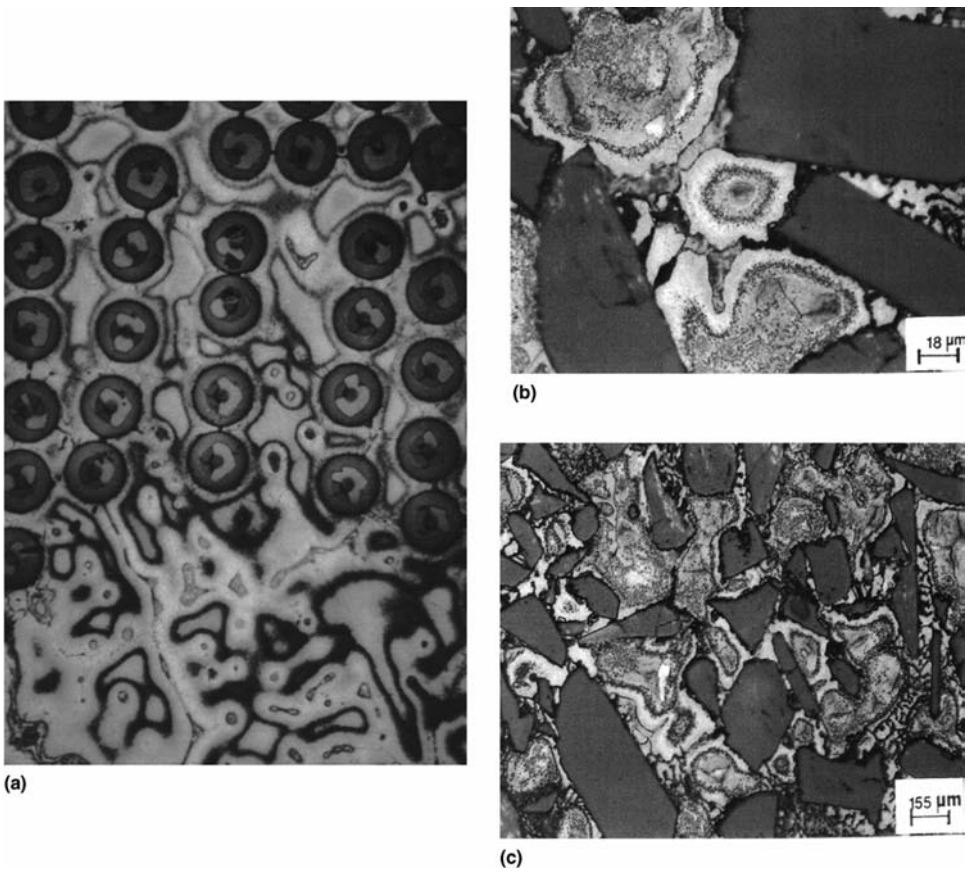

Fig. 3 (a) Transverse section of an SCS-2SiC fiber in an Al-4.5%Cu matrix. (b) and (c) Solidification microstructure of discontinuously reinforced SiC-Al alloy composites showing the influence of the spacing between SiC platelets on microsegregation pattern in aluminum-copper alloys

the secondary dendrite arm spacing in the unreinforced alloy is comparable to interfiber spacing, the grain size becomes large compared to interfiber spacing. In this case, fibers do not enhance the nucleation of the solid phase. With a further decrease in the cooling rates, the extent of microsegregation is reduced, and at sufficiently slow cooling rates, the matrix can be rendered free of microsegregation. The underlying mechanisms range from restricted diffusion in the solid state to dendrite coalescence during solidification (Ref 32–35).

Distribution of Reinforcements

The spatial arrangement of the discontinuous ceramic phase in the cast structure principally determines the properties of the cast composite. The distribution of phases depends on:

- Quality of the melt-particle slurry prior to casting
- Cooling rate
- Viscosity of the solidifying melt
- Shape, size, and volume fraction of particles
- Specific gravities of particles and the melt
- Thermal properties of particles and the matrix alloy
- Chemistry and morphology of crystallizing phases and their interactions with particles
- Nucleation of primary phases on reinforcements
- Entrapment or pushing of particles by solidifying interfaces
- Flocculation of particles and the presence of any external forces during solidification

Figure 5 shows typical microstructures of particle-dispersed composites where the particles are segregated in the last freezing interdendritic regions as a result of pushing by the primary solid. The segregation of particles into the interdendritic regions causes severe agglomeration and interparticle contact, impairing the mechanical properties. Segregation is more severe at smaller particle sizes and at larger dendrite arm spacing (Ref 23).

Research on particle pushing by solidifying interfaces in cast MMCs has been focused on modeling the effects of thermal properties (Ref 24), solute diffusion (Ref 13), gravity, and microgravity (Ref 36). Other areas of focus have included the effects of convection (Ref 37), external fields such as centrifugal force, morphology of the solidification front (Ref 38), and surface energies (Ref 39, 40) (Table 5). Kim and Rohatgi (Ref 41) have proposed models on particle pushing, taking into account the effect of interface shape, which is initially planar, and the presence of solute. The shape of the interface becomes curved after the interaction. The critical interface velocity in a pure melt, above which the particles are engulfed by the moving interfaces, is given by the following equation (Ref 13):

$$V_c = \frac{\Delta\sigma a_0}{18\mu}\left(\frac{kR_1 + 1}{R_1}\right) \qquad \text{(Eq 1)}$$

where $\Delta\sigma$ is the surface energy difference, a_0 is the atomic diameter, μ is the viscosity, k is the curvature of the interface, and R_1 is the particle diameter. During the rejection of particles by growing crystals and pushing of reinforcements ahead of the advancing interface, a viscous force is generated that prevents the pushing of the particle. Therefore, it is the balance of these counteracting forces that determines the rejection or engulfment of the particle. The shape of the solidification front and the magnitude of these forces are affected by several parameters, such as relative density difference, particle size, relative difference in thermal conductivity and heat diffusivity between the particle and the matrix melt, and alloy composition. Figure 6 shows the variation in critical velocity for engulfment as a function of particle size,

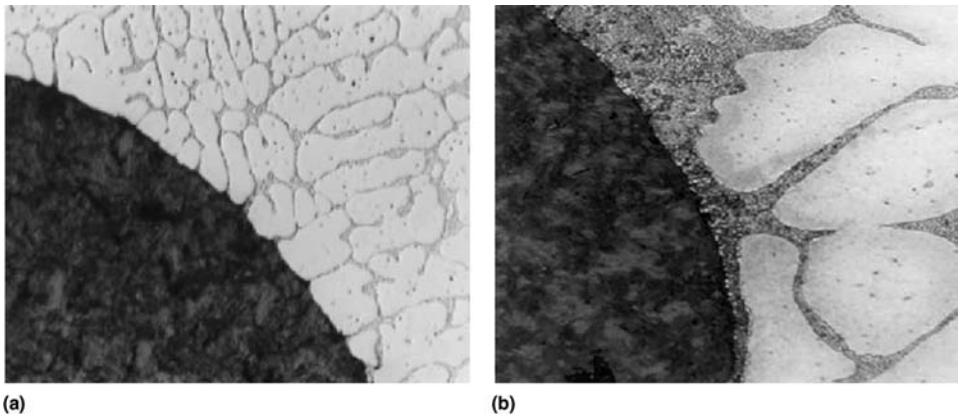

Fig. 4 Solidifying microstructure of thermally managed Al-9%Cu alloy composite (a) with external cooling of graphite rod extending out of the melt and (b) without external cooling of the graphite rod

suggesting that smaller particles will require higher velocities for engulfment.

The interaction between particles and the solidification fronts was observed to lead frequently to segregation of particles in the last freezing interdendritic regions. This happens when the velocity of solidification fronts is lower than the critical interface velocity, an event that depends on various factors, including particle size and its density, melt viscosity, and the shape of the interface and its velocity. An interface velocity greater than the critical interface velocity leads to the engulfment of particles by the interfaces, resulting in a uniform particle distribution due to the presence of the particles within the matrix, an outcome that is likely to greatly enhance the matrix mechanical properties. The critical interface velocities have been experimentally measured in Al-Si/SiC composites; however, it has not been possible to engulf the majority of the reinforcement particles within the dendrites in most conventional casting processes used today (2008).

Modeling of Particle-Pushing Phenomenon

Particle/solidification front interactions in metal-ceramic systems have been modeled using computational methods. The studies showed a distinct difference between the results obtained from a full dynamic analysis and those from previous steady-state analyses (Ref 42–45), particularly when premelting effects were included in the calculations. A significant finding was that when premelting effects are included in the study, the particle pushing/engulfment transition could be determined directly from the dynamics of the problem (Ref 46). The premelted film induced changes in the curvature of the solidification front underneath the particle (i.e., becomes more concave), which promoted engulfment of the particles. Garvin and Udaykumar (Ref 47, 48) computationally examined the drag force acting on the particle as it is approached by the front and quantified its dependence on the thermal conductivities of the particle and the melt.

More recently, Garvin et al. (Ref 49, 50) developed a multiscale method in which they coupled the dynamics of heat and fluid transport at the microscale (i.e., particle scale) with the nanoscale intermolecular interactions acting across the thin melt gap, without imposing any assumptions on the geometry of the front/particle or on the force laws. The solution requires solving a lubrication equation (with disjoining pressure effects for the intermolecular forces included as a body force) for the melt layer and Navier-Stokes equations for the overall particle-front system. The results from these studies allow the critical velocity for particle engulfment to be obtained from the coupled dynamics. The sensitive interaction between the particle and the melt front leads to the determination of the critical velocity for pushing/engulfment in particle-front interactions.

Dendrite and Particle Interaction

In the work of Yang et al. (Ref 51–53), interactions of fronts in undercooled pure melts and directionally solidified (constitutionally supercooled) alloy melts have been studied. These results indicate that the dynamics of particle-front systems in such morphologically unstable situations may be very different from those in the often-studied stable planar solidification front cases. The thermal conductivity ratio of the particle to the melt (k_p/k_l) seems to play an opposite role in the case of an undercooled melt (pure material) versus a directionally solidified pure material (Ref 53). It appears that in dendritic systems with $k_p/k_l < 1$, particles are likely to be engulfed or become trapped in the interdendritic spaces as opposed to being pushed ahead of the front. As a dendrite approaches a particle in an undercooled pure melt, it becomes more convex as k_p/k_l increases. In the directional solidification case of a pure material, the solidification front becomes less convex as k_p/k_l increases.

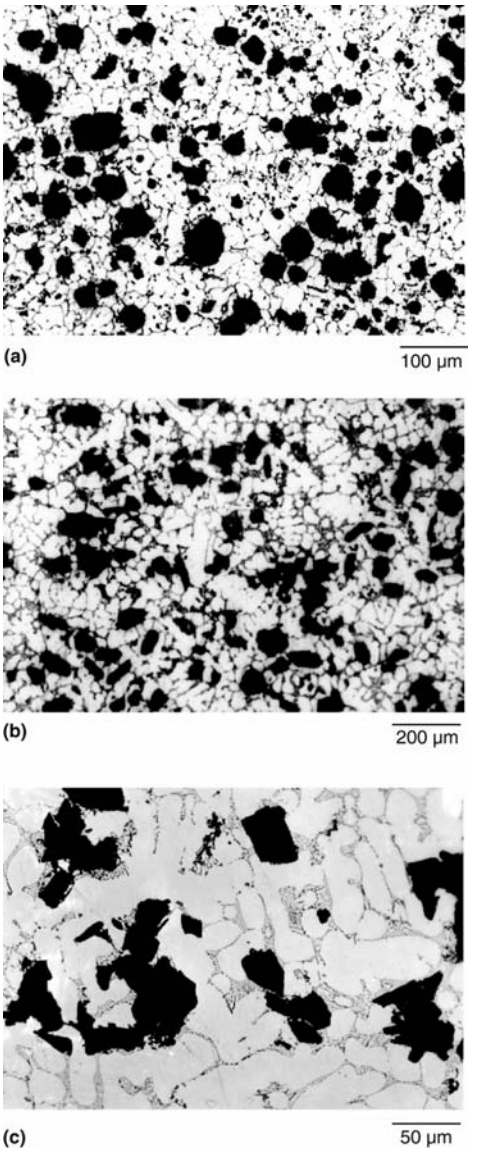

Fig. 5 Microstructures of composites showing pushing of ceramic particulates in the last freezing region liquid. (a) 7074 Al-20vol%Al_2O_3 particle matrix. (b) A356 alloy-based composite with Al_2O_3 (c) A356 alloy-based composite with ZrO_2. Source: Ref 60

Nanoparticles and Solidification Front Interactions

Solidifying interfaces interacting with nanoparticles will likely require a different numerical approach than the ones used for microparticles. The lubrication approach to finding the drag on the particle may not be valid for the case of a nanoparticle. In order for the lubrication theory to hold, the ratio of the gap thickness to the particle radius must be small ($d/R_p \leq 0.1$). In addition, the curvature of the nanoparticle will have a first-order effect on the solidification-front morphology. At high curvatures, the Gibbs-Thomson condition will become very important and tends to flatten the solidifying interface. This will aid in the engulfment of particles.

Table 5 Selected theoretical models of particle pushing

Study	Reported parameters and outcomes
Uhlmann et al.	Repulsive (surface energy) and attractive (viscous drag) forces are introduced; front shape assumed a priori
Bolling and Cisse	More rigorous determination of front shape than Uhlmann et al.; surface roughness considered; introduced gravity and curvature-dependent attractive (drag) force; some ill-defined length scales; obscure nature of rejection force
Hoekstra and Miller	Pushing by ice front modeled; rejection force is due to temperature-dependent transition layer on size; temperature gradient is included
Chernov et al.	Disjoining pressure as repulsive force and fluid drag as attractive force; shape-preserving paraboloidal growth front; considers smooth particles and thermal conductivities of particle and melt; neglects kinetic undercooling; solute screening is considered separately
Stefanescu et al.	Repulsive surface energy and attractive fluid drag; successive approximation-type approach to incorporate thermal conductivities of particle and melt, buoyancy, and volume fraction; a later refinement addresses growth of perturbations on front. Good agreement with some experimental observations
Neumann et al.	Thermodynamic model of pushing; postulates an equation-of-state to determine surface energies. Eminently useful for low-energy (e.g., organic) systems
Gilpin	Disjoining pressure as the repulsive interaction and drag as attractive force; temperature gradient effects included
Catalina and Stefanescu	Proposed a dynamic model of pushing. The model considers acceleration of an initially stationary particle by the front to a steady state at which a thin film is retained. The critical velocity is the limiting velocity at steady state.
Sasikumar et al.	Approach is similar to Chernov et al. but a more rigorous numerical solution of the problem; thermal conductivities of particle and melt are considered; front shape under both steady and nonsteady conditions is determined; assumes repulsive van der Waals and attractive fluid drag forces
Kaptay	Determines conditions for force and spontaneous engulfment by accounting for the interfacial force. Neglects gravity, buoyancy, lift forces, and interfacial energy gradients. Derives an equation for the forces between two solids separated by a thin liquid film
Kim and Rohatgi	Steady-state model of interaction between a spherical particle and a curved interface. Considers thermal conductivity difference between particle and liquid, and the temperature gradient. Also incorporates solute effects in deducing the engulfment velocity
Rempel and Worster	Considers a power law dependence between film thickness and undercooling based on intermolecular interactions. Predicts the interface shape and critical velocity
Hadji	Analyzes the interface instability of a planar front confronted by a particle during unidirectional solidification of dilute suspensions. Defines a segregation coefficient that is modified by particles due to solute and thermal shielding

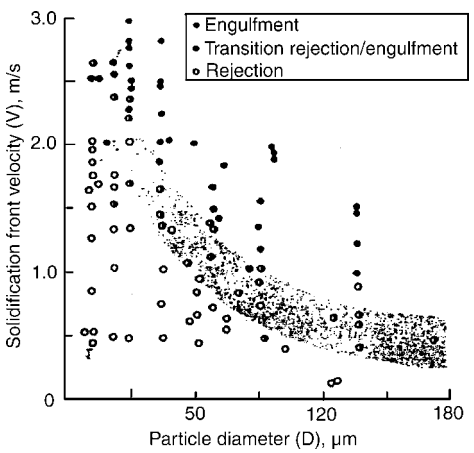

Fig. 6 Variation of the critical interface velocity with particle size

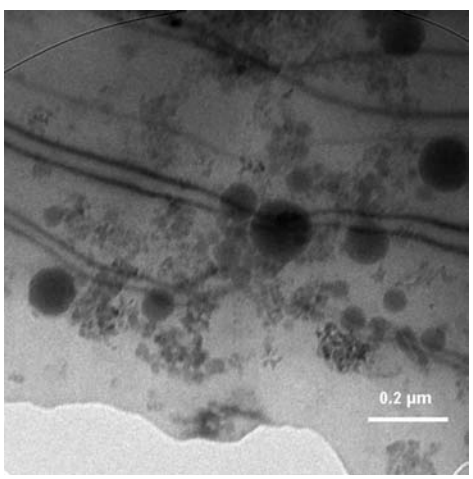

Fig. 7 Transmission electron micrograph of A206/2vol %Al_2O_3 (47 nm) nanocomposite produced by the authors at the University of Wisconsin—Milwaukee

In addition, small particles are more easily pushed; hence, the solidification rates needed to engulf small particles could be quite high (Fig. 6). Brownian motion may also play a role in how a nanoparticle behaves as it interacts with the solidification front. Traditional continuum mechanics approaches may not be applicable for modeling nanoparticles interacting with solidification fronts, due to the small length and time scales. However, molecular dynamics approaches can be applied to such systems. Furthermore, while molecular dynamic calculations can reveal the physics at the nanoscale, a multiscale approach will be necessary to predict the particle distributions at the scales of practical interest, that is, at the macroscale.

Nanocomposites

A variety of metal-matrix nanocomposites (MMNCs) are being developed, with properties that far exceed the limits for metals or composites that contain microscale reinforcements. For example, carbon nanotubes have been shown to exhibit ultrahigh strength and modulus. When included in a matrix, they could impart significant property improvements to the resulting nanocomposite (Ref 54). Solidification processes have been applied for synthesizing nanocomposites (Ref 55). These processes can be divided into three categories: rapid solidification, stir mixing followed by solidification, and infiltration of melt into a preform of reinforcement followed by solidification. Rapid solidification, such as melt spinning, or spray atomization can lead to nanosized grains as well as amorphous metals, from which nanosized reinforcements can be precipitated in the amorphous matrix during heating to form nanocomposites (Ref 56, 57). The stir-mixing methods that have been applied to synthesize MMNCs include use of a high-temperature impeller to stir the melt-reinforcement slurry and use of ultrasonic mixing, where an ultrasonic horn is used to create cavitation in the melt that disperses the particulate reinforcements. Figure 7 shows a microstructure exhibited by a cast nanocomposite synthesized at the University of Wisconsin—Milwaukee (Ref 58, 59). This MMNC was made using a unique method combining the use of stir mixing and ultrasonic mixing, with a wetting agent added to the molten alloy to incorporate nanoparticles in a metallic matrix. This process resulted in the incorporation of nanoparticles within microscale grains of aluminum and formed a bimodal microstructure. Infiltration methods that have been used to cast MMNCs include use of ultrahigh-pressure and pressureless infiltration techniques. In the case of MMNCs, incorporation of as little as 1 vol% of nanosized ceramic particles has led to a much greater increase in the strength and wear resistance of aluminum- and magnesium-matrix composites than was achieved at much higher loading levels of microsized particles. Such improvements have great implications for the automotive, aerospace, and, in particular, defense industries due to the significant weight savings and exceptional properties that can be achieved.

Conclusions

- Considerable progress has been made in the field of cast MMCs since cast aluminum-graphite particle composites were first synthesized in 1965. Stir mixing and casting as well as pressure infiltration have emerged as the two major processes to make composites.
- Presence of reinforcements in the melt influences solidification of castings in several ways, including the changes in the patterns of microsegregation that can reduce the heat treatment time required for castings. The knowledge base in the solidification of MMCs has enhanced the understanding of solidification of monolithic castings.

- MMCs have unique properties, including high specific strength, high specific modulus, wear resistance, low coefficient of thermal expansion, and high specific conductivity, which make them very attractive for automotive, electronic packaging, and space applications.
- Several MMC components are currently being used as automotive components, such as brake rotors, pistons, cylinder liners, drive shafts, and engine pulleys. They are also used in aerospace applications such as space shuttle orbiter struts, antenna wave-guide mast, microwave thermal packaging, power semiconductor base, ventral fins, eurocoptor blade sleeves, fuel access doors, and fan exit guide vanes.
- Emerging cast MMCs with considerable potential include aluminum-graphite, aluminum-fly ash, aluminum-silicon carbide-graphite, lead-free copper-graphite, and open-cell and syntactic composite foams.
- There are several research challenges in the field of cast MMCs, including development of special matrices and reinforcements, decreasing the cost and facilitating machining of composites, and generating handbook-grade data for design. Several fundamental issues include nucleation and growth amid reinforcements and interactions between solidifying interfaces. Micro- and nanosized reinforcements need further investigation to achieve the desired distribution of reinforcements in cast composites.
- In the future, the technology of casting MMCs can enable foundries to produce higher-performance castings and other advanced materials, including functionally gradient materials, nanocomposites, smart composites, biomedical implants, superconducting composites, and porous and cellular solids.
- There are exciting opportunities for producing exceptionally strong, wear-resistant cast MMNCs with acceptable ductility by solidification processing. However, low-cost bulk processing methods must be developed to synthesize these materials with little to no voids or defects and with improved ductility.

ACKNOWLEDGMENT

Nikhil Gupta would like to acknowledge the National Science Foundation grant CMMI0726723. The authors thank Dr. Justin Garvin at the Air Force Research Laboratory for useful discussions.

REFERENCES

1. A. Banerjee, M.K. Surappa, and P.K. Rohatgi, Preparation and Properties of Cast Aluminum Alloy-Zircon Particle Composites, *Metall. Trans. B,* Vol 14, 1983, p 273
2. P.K. Rohatgi, B.C. Pai, and S.C. Panda, Preparation of Cast Aluminum-Silica Particulate Composites, *J. Mater. Sci.,* Vol 14, 1979, p 2277
3. M.K. Surappa and P.K. Rohatgi, Preparation and Properties of Cast Aluminum-Ceramic Particle Composites, *J. Mater. Sci.,* Vol 16, 1981, p 983
4. D. Nath, R.T. Bhat, and P.K. Rohatgi, Preparation of Cast Aluminum Alloy-Mica Particle Composites, *J. Mater. Sci.,* Vol 15, 1980, p 1241
5. F.A. Badia and P.K. Rohatgi, Dispersion of Graphite Particles in Aluminum Castings Through Injection of the Melt, *Trans. AFS,* Vol 77, 1969, p 402
6. B.C. Pai and P.K. Rohatgi, Production of Cast Aluminum-Graphite Particle Composites Using a Pellet Method, *J. Mater. Sci.,* Vol 13, 1978, p 329
7. P.K. Rohatgi, R. Asthana, and S. Das, Solidification, Structures and Properties of Cast Metal-Ceramic Particle Composites, *Int. Met. Rev.,* Vol 31, 1986, p 115–139
8. M. Emamy, A. Razaghian, H.R. Lashgari, and R. Abbasi, The Effect of Al-5Ti-1B on the Microstructure, Hardness and Tensile Properties of Al_2O_3 and SiC-Containing Metal-Matrix Composites, *Mater. Sci. Eng. A,* Vol 485 (No. 1–2), 2008, p 210–217
9. H.A. Katzman, Carbon-Reinforced Metal-Matrix Composites, U.S. Patent 4,376,808, 1983
10. D.M. Schuster, M.D. Skibo, and W.R. Hoover, *Light Met. Age,* Feb. 15, 1989
11. M.A. Liquin, C. Feng, and S. Guangji, *J. Mater. Sci. Lett.,* Vol 14, 1995, p 649
12. V.G. Gorbunov, V.D. Parshin, and V.V. Panin, *Russ. Cast Product.,* Vol 8 1971, p348
13. J.K. Kim and P.K. Rohatgi, An Analytical Solution of the Critical Interface Velocity for the Encapture of Insoluble Particles by a Moving Solid-Liquid Interface, *Metall. Mater. Trans. A,* Vol 29, 1998, p 351–358
14. Alcan Aluminum Corporation (Duralcan), U.S. Patent 4,786,467, 1988
15. T. Sridharan, Extended Abstract of Conference on Metal-Matrix Composites: Property Optimization and Application, U.K. IOM, 1989
16. A. Mortensen, J.A. Cornie, and M.C. Flemings, *JOM,* Vol 40 (No. 2), 1988, p 12
17. H. Fukunaga and K. Goda, *Bull. JSME (Japan),* Vol 28, 1985, p 235
18. A.A. Das and S. Chatterjee, *Metall. Mater. Technol,* March 1981, p137
19. P.S. Cook and P.S. Werner, *Mater. Sci. Eng. A,* Vol 144, 1991, p 189
20. S.K. Verma and J.L. Dorcic, *Cast Reinforced Metal Composites,* S.G. Fishman and A.K. Dhingra, Ed., ASM International, 1988, p115
21. Y. Kun, V. Dollhopf, R. Kochendorfer, *Compos. Sci. Technol.,* Vol 46, 1993, p1
22. J. Yang and D.D.L. Chung, *J. Mater. Sci.,* Vol 24, 1989, p3605
23. L. Kurian and R. Sasikumar, *Acta Metall. Mater.,* Vol 40, 1992, p 2375
24. D.M. Stefanesfu and B.K. Dhindaw, Behavior of Insoluble Particles at the Solid-Liquid Interface, *Casting,* Vol 15, Metals Handbook, 9th ed., ASM International, 1988, p 142–147
25. E. Breval, M.K. Aghajanian, J.P. Biel, and S. Anolin, *J. Am. Ceram. Soc.,* Vol 76 (No. 7), 1993, p1865
26. M.K. Aghajanian and J.T. Burke, in *Tomorrow's Materials Today*, SAMPE series, Vol 34, 1989, p 817
27. Y. Liu, P.K. Rohatgi, and S. Ray, Tribological Characteristics of Aluminum-50 vol pct Graphite Composite, *Metall. Mater. Trans. A,* Vol 24 (No. 1), 1993, pp 151–159
28. O. Couteau and D.C. Dunand, Creep of Aluminum Syntactic Foams, *Mater. Sci. Eng. A,* Vol 488 (No. 1–2), 2008, p 573–579
29. P.K. Rohatgi, C.S. Narendranath, and D. Wang, in *Microstructure Formation during Solidification of Metal Matrix Composites,* P.K. Rohatgi, Ed., TMS, 1992, p 149–160
30. A. Mortensen, M.N. Gungor, J.A. Cornie, and M.C. Flemings, Alloy Microstructure in Cast Metal-Matrix Composites, *J. Met.,* March 1986, p 30
31. R. Asthana and P.K. Rohatgi, *Z. Metallkd.,* Vol 84, 1993, p 44
32. H. Nakae and S.Wu, *Key Eng. Mater.,* Vol 127–131, 1997, p503
33. J.A. Cornie, A. Mortensen, M. Gungor, and M.C. Flemings, The Solidification Process During Pressure Casting SiC and Al_2O_3 Reinforced Al-4.5% Cu Metal-Matrix Composites, *Proceedings of the Fifth International Conference on Composite Materials (ICCM-V),* W.C. Harrigan, J. Strife, and A.K. Dhingra, Ed., American Institute of Mining, Metallurgical, and Petroleum Engineers, 1985, p 809
34. L.J. Masur, A. Mortensen, J.A. Cornie, and M.C. Flemings, Pressure Casting of Fiber Reinforced Metals, *Proceedings of the Sixth International Conference on Composite Materials (ICCM-VI),* American Institute of Mining, Metallurgical, and Petroleum Engineers, 1987
35. A. Mortensen, M.C. Flemings, and J.A. Cornie, "Columnar Dendritic Solidification in a Metal-Matrix Composite," Annual Report of the Centre for the Processing and Evaluation of Metal and Ceramic Matrix Composites, Massachusetts Institute of Technology, Feb 1987
36. D.M. Stefanescu, F.R. Juretzko, B.K. Dhindaw, A. Cartalina, S. Sen, and P.A. Curreri, Particle Engulfment and Pushing by Solidifying Interfaces, Part I: Microgravity Experiments and Theoretical Analysis, *Metall. Mater. Trans. A,* Vol 29, 1998, p 1697–1706
37. S. Sen, B.K. Dhindaw, A. Catalina, D.M. Stefanescu, and P.A. Curreri, Melt Convection Effects on the Critical Velocity of Particle Engulfment, *J. Cryst. Growth,* Vol 173, 1997, p 574–584
38. J.A. Sekhar and R. Trivedi, Solidification Microstructure Evolution in the Presence of Inert Particles, *Mater. Sci. Eng. A,* Vol 147, 1991, p 9

39. A.W. Neumann, R.J. Good, C.J. Hope, and M. Sejpal, An Equation of State Approach to Determine Surface Tensions of Low Energy Solids from Contact Angle, *J. Colloid Interface Sci.,* Vol 69 (No. 2), 1974, p 291–302
40. R. Asthana and S.N. Tewari, *Compos. Manuf.,* Vol 4, 1993 p 3
41. J.K. Kim and P.K. Rohatgi, The Effect of the Diffusion of Solute between the Particle and the Interface on the Particle Pushing Phenomenon, *Acta Metall. Mater.,* Vol 46 (No. 4), 1998, p 1115–1123
42. G.F. Bolling and J. Cisse, A Theory for the Interaction of Particles with a Solidifying Front, *J. Cryst. Growth,* Vol 10, 1971, p 56–66
43. A.A. Chernov, D.E. Temkin, and A.M. Mel'nikova, Theory of the Capture of Solid Inclusions during the Growth of Crystals from the Melt, *Sov. Phys. Crystallogr.,* Vol 21 (No. 4), 1976, p 369–373
44. D.K. Shangguan, S. Ahuja, and D.M. Stefanescu, An Analytical Model for the Interaction between an Insoluble Particle and an Advancing Solid/Liquid Interface, *Metall. Mater. Trans. A,* Vol 23, 1992, p 669–680
45. A.W. Rempel and M.G. Worster, The Interaction between a Particle and an Advancing Solidification Front, *J. Cryst. Growth,* Vol 205, 1999, p 427–440
46. J.W. Garvin and H.S. Udaykumar, Effect of a Premelted Film on the Dynamics of Particle-Solidification Front Interactions, *J. Cryst. Growth,* Vol 290 (No. 2), May 2006, p 602–614
47. J.W. Garvin and H.S. Udaykumar, Drag on a Particle Being Pushed by a Solidification Front and Its Dependence on Thermal Conductivities, *J. Cryst. Growth,* Vol 267 (No. 3–4), July 2004, p 724–737
48. J.W. Garvin and H.S. Udaykumar, Drag on a Ceramic Particle Being Pushed by a Metallic Solidification Front, *J. Cryst. Growth,* Vol 276 (No. 1–2), March 2005, p 275–280
49. J.W. Garvin, Y. Yang, and H.S. Udaykumar, Multiscale Modeling of Particle-Solidification Front Dynamics, Part I: Methodology, *Int. J. Heat Mass Trans.,* Vol 50 (No. 15–16), July 2007, p 2952–2968
50. J.W. Garvin, Y. Yang, and H.S. Udaykumar, Multiscale Modeling of Particle-Solidification Front Dynamics, Part II: Pushing-Engulfment Transition, *Int. J. Heat Mass Transf.,* Vol 50 (No. 15–16), July 2007, p 2969–2980
51. Y. Yang and H.S. Udaykumar, Sharp Interface Cartesian Grid Method, Part III: Solidification of Pure Materials and Binary Solutions, *J. Comput. Phys.,* Vol 210 (No. 1), Nov 2005, p 55–74
52. Y. Yang, J.W. Garvin, and H.S. Udaykumar, Sharp Interface Numerical Simulation of Directional Solidification of Binary Alloy in the Presence of a Ceramic Particle, *Int. J. Heat Mass Transf.,* Vol 51 (No. 1–2), Jan 2008, p 155–168
53. Y. Yang, J.W. Garvin, and H.S. Udaykumar, Sharp Interface Simulation of Interaction of a Growing Dendrite with a Stationary Solid Particle, *Int. J. Heat Mass Transf.,* Vol 48 (No. 25–26), Dec 2005, p 5270–5283
54. J.P. Salvetat, G. Andrew, D. Briggs, T.M. Bonard, R.R. Basca, and A.J. Kulik, *Phys. Rev. Lett.,* Vol 82, 1999, p 944
55. P. Rohatgi, N. Gupta, and B. Schultz, submitted to *Int. Mater. Rev.,* 2007
56. S.F. Hassan, and M. Gupta, *J. Alloy. Compd.,* Vol 429, 2007, p 176
57. B. Cantor, *J. Metastable Nanocryst. Mater.,* Vol 1, 1999, p 143
58. B.F. Schultz and P.K. Rohatgi, Structure and Properties of a Stir Cast Aluminum Alloy A206-Al_2O_3 Nanoparticles Composite, submitted to *Mater. Sci. Eng. A,* 2007
59. B.F. Schultz, P.K. Rohatgi, S. Alaraj, and J.B. Ferguson, Influence of Processing Parameters on the Hardness of A206 Alloy-Al_2O_3 Nanoparticle Composites, submitted to *Compos. Sci. Technol.,* 2007
60. A. Daoud, M. Abo-Elkhar, *Journal of Material Processing Technology,* Volume 120, Issues 1–3, 15 Jan 2002, p 296–302